Solid State Communications 280 (2018) 50–55

Contents lists available at ScienceDirect

Solid State Communications

journal homepage: www.elsevier.com/locate/ssc

Communication

Surface plasmon characteristics based on graphene-cavity-coupled waveguide system

Zhaohui Chen[a], Renlong Zhou[a,b,*], Lingxi Wu[a], Sa Yang[b,**], Dan Liu[b]

[a] School of Physics and Electronic Science, Hunan University of Science and Technology, Xiangtan 411201, PR China
[b] School of Physics and Information Engineering, Guangdong University of Education, Guangzhou 510303, PR China

ARTICLE INFO

Communicated by F. Peeters

Keywords:
Graphene nanoribbon
Surface plasmon
Fermi level

ABSTRACT

We theoretically investigate the localized surface plasmon of graphene in graphene-cavity-coupled waveguide system with using finite-difference time-domain (FDTD) method and the coupled mode theory (CMT). Cavity provides the strong light-matter interaction between graphene and light. And strongly confined radiation can be confined in a thin and finite width graphene. The fermi level of the graphene nanoribbon plays an important role in tuning the graphene surface plasmon. The faint high-order mode of graphene surface plasmon is also observed. The resonant wavelengths of graphene surface plasmon are almost unaffected by the altering of the refractive index of the cavity core, susceptibility of the cavity core and intensity of incident light. This paper can give an insight of the localized surface plasmon properties in graphene system or any other 2D system. And graphene assisted with cavity is an attractive candidate for designing active graphene plasmonic devices or any other 2D plasmonic devices.

1. Introduction

Surface plasmons (SPs) are the electromagnetic waves that spread on the surface of a conductor because of the interaction between the light waves, electromagnetic field in dielectric and the free electrons of the conductor [1]. Since the SPs can overcome the diffraction limit and manipulate light in nanoscale domain, nanodevices have extraordinary properties, such as high miniaturization and integration. Recently, surface plasmons pave the way to some important applications in areas such as sensing [2], waveguides [3,4], absorbers [5–7] and other optical modulators [8,9]. Considering SPs' properties, nanoscale plasmon resonator system has been illustrated theoretically and experimentally in recent researches [10,11]. However, very few qualitative descriptions have been showed on graphene surface plasmons (GSPs).

Recently, graphene, a two-dimensional (2D) form of carbon in which the atoms are arranged in a honeycomb lattice [12], has shown its promising potentials in photonics and optoelectronic applications because of its unique band structures of Dirac Fermions. Graphene provides a suitable alternative to plasmons, because it exhibits much larger confinement and much longer propagation distances. It is demonstrated that the altering of the graphene's physical parameters [13,14] leads to a dramatic change in optical properties of graphene. Plasmons in graphene provide more potential for optical applications as well [15–21]. The distinguishing from other thin materials is that graphene possess better properties than other thin material. Firstly, graphene possess extreme electromagnetic confinement. Secondly, the graphene has relatively low loss. Lastly, graphene has dynamic tunability with fermi level by changing the doping level via the electrostatic or chemical gating. So we consider graphene and not any other thin film material. Single layer graphene only has the optical absorptivity about 2.3%. With the resonance effect between graphene and cavity, the absorptivity of graphene can be increased [22]. The absorption for any other 2D material can also be enhanced due to interaction between 2D material and cavity. Like the metal, graphene nanoribbons (GNR) are expected to play an important role in surface plasmons. However, it is still a challenge to achieve strong confinement of the graphene surface plasmons (GSPs).

In this paper, we numerically and theoretically investigate the propagation of surface plasmons in graphene system. It has strong light-matter interaction between graphene and light due to the assisted cavity resonance. The thin graphene can confine radiation in finite width size. The consistency between the analytical model and the finite-difference time-domain (FDTD) method validates the feasibility of the theoretical analysis. Graphene surface plasmons (GSPs) can be effectively tuned by changing the fermi level of the graphene nanoribbon and the length of graphene-cavity. The graphene modes of graphene

* Corresponding author. School of Physics and Electronic Science, Hunan University of Science and Technology, Xiangtan 411201, PR China.
** Corresponding author.
E-mail addresses: rlzhou@mail.sitp.ac.cn (R. Zhou), yangs7014@sina.com (S. Yang).

https://doi.org/10.1016/j.ssc.2018.06.006
Received 2 February 2018; Received in revised form 31 May 2018; Accepted 13 June 2018
Available online 14 June 2018
0038-1098/

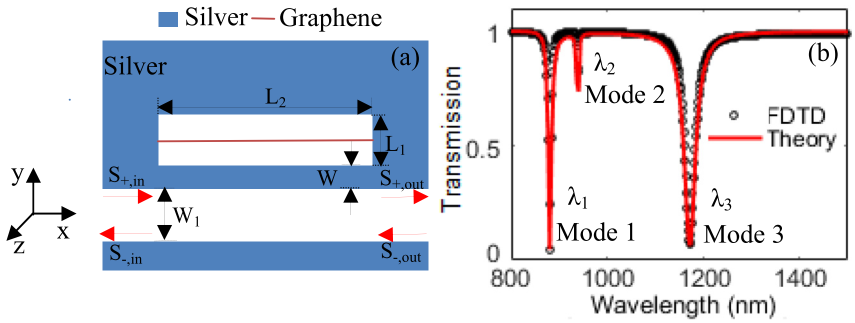

Fig. 1. (a) The schematic of graphene system. (b) The transmission spectra with using the FDTD simulation (black circles line) and the CMT theory (red solid line). (For interpretation of the references to colour in this figure legend, the reader is referred to the Web version of this article.)

system have been seldom influenced by the altering of refractive index of the cavity core, susceptibility $\chi^{(3)}$ and intensity of incident light, while the cavity mode is affected a bit more. The plasmon properties of graphene system are also discussed here.

2. The model and theoretical analysis

The schematic illustration of graphene system is shown in Fig. 1(a). The system consists of an MDM waveguide, a cavity and a graphene nanoribbon. Cavity has the parameters with length $L_2 = 400$ nm and width $L_1 = 100$ nm. The position of graphene nanoribbon is in the center of cavity along y-axis direction. The length of graphene nanoribbon L_2 is 400 nm. The permittivity of the silver can be determined by the Drude model, which defines as $\varepsilon(\omega) = \varepsilon_\infty - \omega_p^2/(\omega^2 + i\omega\gamma)\frac{n!}{r!(n-r)!}$, where ω stands for the angle frequency of the incident wave, the dielectric constant at the infinite frequency $\varepsilon_\infty = 3.7$, the plasma frequency $\omega_p = 1.38 \times 10^{16}$rad/s and the damping rate $\gamma = 2.73 \times 10^{13}$rad/s. The gap w between the MDM waveguide and cavity is 20 nm. The other structure parameters are the thickness of the graphene nanoribbon (d = 1 nm) [22,23] and the width of waveguide ($w_1 = 100$ nm). The graphene is treated as an ultrathin film layer with a thickness of d. Here, d is not the real thickness of graphene and reasonably set to be 1 nm. The dielectric in the waveguide and cavity is air. In the mid-infrared spectral region, the optical feature of graphene can be conveyed by the surface conductivity σ_{gra} [22,23]:

$$\sigma_{gra}(\omega) = ie^2E_f/[\pi\hbar^2(\omega + i\tau^{-1})] \tag{1}$$

Here, e is electric charge, $\hbar$ is Planck's constant. The lifetime is $\tau = (\mu E_f)/(e v_f{}^2)$, μ is carrier mobility, E_f is fermi level, v_f is fermi velocity. The parameters of the graphene are set as $v_f = 10^6$ m/s, $\mu = 1\text{m}^2/(\text{V·s})$, and $E_f = 0.64$ eV.

The third-order nonlinear dielectric material is used to fill up the cavity, whose electric constant can be characterized by ε_d. Under the nonlinear situation, the dielectric constant ε_k of the kerr material depends on the intensity of electric field, which can be expressed as: $\varepsilon_k = \varepsilon_d + \chi^{(3)}|E|^2$, where the linear refractive index ε_d is chosen as 1.0. The third-order nonlinear susceptibility is chosen to be $\chi^{(3)} = 10^{-14}\,\text{m}^2/\text{V}^2$, and $\varepsilon_d = n_d{}^2$.

The TM-polarized plane wave is emitted from the left port of the plasmonic waveguide and propagates along x-axis direction. In order to model the transmission properties of the structure, the method of perfect matching layer (PML) boundary condition is adopted.

As the TM-polarized plane waves pass through the MDM waveguide, the energy can be coupled into the cavity and graphene nanoribbon. The dynamic transmission characteristics of the proposed structure can be investigated by the CMT. As shown in Fig. 1(a), the incoming and outgoing waves in the resonators are depicted by $S_{\pm,\,in}$ and $S_{\pm,\,\text{out}}$. The subscript ± represent two propagating directions of waveguide as shown in Fig. 1(a). A_1, A_2 and A_3 denote the energy amplitude of resonant mode 1, resonant mode 2, and resonant mode 3, respectively. Thus, the energy amplitude of three resonant modes with corresponding frequency ω_i $(i = 1,\ 2,\ 3)$ can be expressed as

$$\frac{dA_1}{dt} = \left(-i\omega_1 - \frac{1}{\tau_{i1}} - \frac{1}{\tau_{w1}}\right)A_1 + S_{+,in}\sqrt{\frac{1}{\tau_{w1}}} + S_{-,in}\sqrt{\frac{1}{\tau_{w1}}} - i\mu_{12}e^{j\phi_1}A_2 - i\mu_{13}e^{j\phi_3}A_3 \tag{2}$$

$$\frac{dA_2}{dt} = \left(-i\omega_2 - \frac{1}{\tau_{i2}} - \frac{1}{\tau_{w2}}\right)A_2 + S_{+,in}\sqrt{\frac{1}{\tau_{w2}}} + S_{-,in}\sqrt{\frac{1}{\tau_{w2}}} - i\mu_{21}e^{j\phi_1}A_1 - i\mu_{23}e^{j\phi_2}A_3 \tag{3}$$

$$\frac{dA_3}{dt} = \left(-i\omega_3 - \frac{1}{\tau_{i3}} - \frac{1}{\tau_{w3}}\right)A_3 + S_{+,in}\sqrt{\frac{1}{\tau_{w3}}} + S_{-,in}\sqrt{\frac{1}{\tau_{w3}}} - i\mu_{32}e^{j\phi_2}A_2 - i\mu_{31}e^{j\phi_3}A_1 \tag{4}$$

Where $\omega_n(\lambda_n)$ (N = 1, 2, 3) is the resonant frequency(wavelength) of three resonant modes, $1/\tau_{iN} = \omega_N/(2Q_{iN})$ is the decay rate due to intrinsic loss in the mode N (N = 1, 2, 3), $1/\tau_{\omega N} = \omega_N/(2Q_{\omega N})$ is the decay rate due to energy escaping into the MDM waveguide. $\mu_{21} = \mu_{31} = \omega_1/(2Q_c)$, $\mu_{12} = \mu_{32} = \omega_2/(2Q_c)$ and $\mu_{23} = \mu_{13} = \omega_3/(2Q_c)$ are the coupling coefficients among three resonant modes. Q_{iN}, $Q_{\omega N}$ are cavity quality factors related to intrinsic loss and waveguide coupling loss. $Q_c = \lambda_n/\Delta\lambda_n$ is the quality factor of resonant mode n (n = 1, 2, 3). Thus, we can get the following formulation:

$$S_{+,out} = S_{+,in} - \sqrt{\frac{1}{\tau_{\omega 1}}}A_1 - \sqrt{\frac{1}{\tau_{\omega 2}}}A_2 - \sqrt{\frac{1}{\tau_{\omega 3}}}A_3 \tag{5}$$

$$S_{-,\text{out}} = S_{-,in} - \sqrt{\frac{1}{\tau_{\omega 1}}}A_1 - \sqrt{\frac{1}{\tau_{\omega 2}}}A_2 - \sqrt{\frac{1}{\tau_{\omega 3}}}A_3 \tag{6}$$

Using boundary conditions of $S_{-,in}^{(2)} = 0$ and Eqs. (4)–(5), we finally achieve the transfer function of the system,

$$t = \frac{S_{+,out}}{S_{+,in}} = 1 - \sqrt{\frac{1}{\tau_{w1}}}A - \sqrt{\frac{1}{\tau_{w2}}}B - \sqrt{\frac{1}{\tau_{w3}}}C \tag{7}$$

Where, $\gamma_1 = i\omega - i\omega_1 - 1/\tau_{i1} - 1/\tau_{\omega 1}$, $\gamma_2 = i\omega - i\omega_2 - 1/\tau_{i2} - 1/\tau_{\omega 2}$, $\gamma_3 = i\omega - i\omega_3 - 1/\tau_{i3} - 1/\tau_{\omega 3}$, $\chi_1 = i\mu_{12}e^{j\phi_1}$, $\chi_2 = i\mu_{13}e^{j\phi_3}$, $\chi_3 = i\mu_{21}e^{j\phi_1}$, $\chi_4 = i\mu_{23}e^{j\phi_2}$, $\chi_5 = i\mu_{31}e^{j\phi_3}$, $\chi_6 = i\mu_{32}e^{j\phi_2}$. A, B and C denote three different physical parameters. Thus, the transmission coefficient is $T = |t|^2$. It is evidently that the transmission spectra with the theoretical results (black cycles line) are in good agreement with the FDTD simulations (red solid lines) as shown in Fig. 1(b). The resonant modes at the resonant wavelengths $\lambda_1 = 887$ nm, $\lambda_2 = 945$ nm and $\lambda_3 = 1185$ nm are called resonant mode 1, resonant mode 2, resonant mode 3, respectively.

For the sake of visualizing three resonant modes more clearly, the distributions of amplitude for electric fields ($|E_y|$) at the resonant wavelengths $\lambda_1 = 887$ nm, $\lambda_2 = 945$ nm and $\lambda_3 = 1185$ nm are depicted in Fig. 2(a)–(c). It is evidently that the electric field amplitude ($|E_y|$) at the resonant wavelength $\lambda_1 = 887$ nm is strongly confined in graphene